

The impact of nebular emission on the ages of $z \approx 6$ galaxies

D. Schaerer^{1,2} and S. de Barros¹

¹ Geneva Observatory, University of Geneva, 51 Ch. des Maillettes, 1290 Versoix, Switzerland
e-mail: daniel.schaerer@unige.ch

² Laboratoire d'Astrophysique de Toulouse-Tarbes, Université de Toulouse, CNRS, 14 Avenue E. Belin, 31400 Toulouse, France

Received 3 February 2009 / Accepted 27 April 2009

ABSTRACT

Aims. We examine the influence of nebular continuous and line emission in high-redshift star forming galaxies on determinations of their age, formation redshift, and other properties from SED fits.

Methods. We include nebular emission consistently with the stellar emission in our SED fitting tool and analyse differentially a sample of 10 $z \approx 6$ galaxies in the GOODS-S field studied earlier elsewhere.

Results. We find that the apparent Balmer/4000 Å breaks observed in a number of $z \approx 6$ galaxies detected at $\geq 3.6 \mu\text{m}$ with IRAC/Spitzer can be mimicked by the presence of strong restframe optical emission lines, implying in particular younger ages than previously thought. Applying these models to the small sample of $z \approx 6$ galaxies, we find that this effect may lead to a typical downward revision of their stellar ages by a factor ~ 3 . In consequence their average formation redshift may be reduced drastically, and these objects may not have contributed to cosmic reionisation at $z > 6$. Extinction and stellar mass estimates may also be somewhat modified, but to a lesser extent.

Conclusions. Careful SED fits including nebular emission and treating properly uncertainties and degeneracies are necessary for more accurate determinations of the physical parameters of high- z galaxies.

Key words. galaxies: starburst – galaxies: high-redshift

1. Introduction

Although star-forming, high-redshift galaxies have been identified out to redshift $z \gtrsim 6$, little is known about the physical properties of these galaxies, since this requires sensitive observations in the near-IR range and beyond. With the advent of Spitzer it has recently become possible to detect galaxies at $z \sim 6-7$ at wavelengths $\geq 3.6 \mu\text{m}$, albeit still in quite small numbers (Egami et al. 2005; Eyles et al. 2005; Yan et al. 2005, 2006; Eyles et al. 2007). One of the main surprises of these studies has been finding a substantial Balmer/4000 Å spectral break in a large fraction of these objects, taken as indicating the presence of an “old” (several hundred Myr) underlying stellar population, which would indicate very high formation redshifts for these galaxies. For example, at $z \approx 6$, Yan et al. (2006) estimate representative ages of 40–500 Myr for their sample of ~ 50 IRAC detected objects, and Eyles et al. (2007) analyse 10 IRAC detected galaxies and derive ages of $\sim 200-700$ Myr and corresponding $7 \leq z_{\text{form}} \leq 18$. However, it is possible that the Balmer break is affected or mimicked by emission lines in high- z galaxies with intense star formation, since their contribution to photometric filters increases with $(1+z)$ (see e.g. Schaerer & Pelló 2005). Determining properties such as maximum ages, past star formation histories, and formation redshifts is important for a variety of topics including our knowledge of galaxy formation, our understanding of cosmic reionisation and its sources, and others. It is therefore essential to thoroughly examine the uncertainties in the underlying SED analysis.

While possible uncertainties in stellar mass estimates of high- z galaxies have the focus of several recent discussions (see e.g. Maraston et al. 2006; Bruzual 2007; Elsner et al. 2008), little attention has been paid to the impact of nebular emission (both

lines and continuous emission) on SED analysis, since these processes are usually not included in evolutionary synthesis models. The effect of nebular emission on broad-band photometry of galaxies has been studied in several papers (e.g. Anders & Fritze-v. Alvensleben 2003; Zackrisson et al. 2008), and it leads to improvements for photometric redshifts, as shown recently by Ilbert (2009) and Kotulla & Fritze (2009). Nevertheless, such models have so far not been applied to analysing the properties of high- z galaxies (but see Raiter et al. 2009). Here, we examine in a differential manner the effect of nebular emission on $z \approx 6$ galaxies, and we show that it can have a significant impact on determinations of their age, and hence on their formation redshift.

In Sect. 2 we summarise the galaxy sample and the SED fitting method. Our results and their implications are presented in Sect. 3. Our main conclusions are discussed and summarised in Sect. 4. We assume a flat Λ CDM cosmology with $H_0 = 70 \text{ km s}^{-1} \text{ Mpc}^{-1}$, $\Omega_M = 0.3$, and $\Omega_{\text{vac}} = 0.7$.

2. Observational data and modelling tools

2.1. Selection of $z \approx 6$ galaxies

To examine the robustness of stellar ages and other physical parameters of the most distant galaxies, we chose the sample of ten $z \approx 6$ star-forming galaxies from the GOODS-South field modelled earlier by Eyles et al. (2007, hereafter E07). Four of these objects have spectroscopic redshifts determined from their Ly α emission; for the remaining objects we use the photometric redshifts from the GOODS-MUSIC catalogue adopted by E07. We use the $i'z'JK_s$, $3.6 \mu\text{m}$, and $4.5 \mu\text{m}$ ACS, ISAAC, and IRAC photometry from E07.

Since longer wavelength data is also available, we also used for comparison the IRAC photometry at 5.8 and 8.0 μm from the GOODS-MUSIC catalogue of Grazian et al. (2006) for the subsample of 3 objects with spectroscopic redshifts also covered by their data.

2.2. SED fitting tool

In analysing the SEDs we use a modified version of the *Hyperz* photometric redshift code of Bolzonella et al. (2000) described, e.g., in Schaerer & Pelló (2005) and Schaerer et al. (2007) and adapted to include nebular emission. Among the large choice of spectral templates included in this version, we here use the 2003 GALAXEV synthesis models from Bruzual & Charlot (2003), covering different metallicities and a wide range of star formation (SF) histories (bursts, exponentially decreasing, or constant SF). For comparison with E07, we define the stellar age t_* as the age since the onset of star formation, we adopt a Salpeter IMF from 0.1 to 100 M_\odot , and we properly treat the returned ISM mass from stars.

To account for the effects of nebular emission from young, massive stars on the SED, we include nebular emission (both lines and continua) in a simple manner. Continuum emission is added to the stellar SED, as in our synthesis models (cf. Schaerer & Vacca 1998; Leitherer et al. 1999; Schaerer 2003). The main emission lines of He, C, N, O, S, and other lines are included using the empirical relative line intensities compiled by Anders & Fritze-v. Alvensleben (2003) from galaxies grouped in three metallicity intervals covering $\sim 1/50 Z_\odot$ to Z_\odot ¹. In addition, we include H recombination lines from the Balmer, Paschen, and Brackett series, as well as Ly α ; their relative intensities are taken from Storey & Hummer (1995) for a typical ISM (density, temperature) of ($n_e = 100 \text{ cm}^{-3}$, 10^4 K)². The absolute strength of both the continuous and line emission depend to first order only on the total number of Lyman continuum photons, which can be computed from the template stellar SED. In this manner we include the main nebular emission features from the UV (Ly α) to 2 μm (restframe), necessary for fitting the SED of galaxies at $z > 4$ up to 10 μm (IRAC Channel 4).

The free parameters of our SED fits are: the metallicity Z (of stars and gas), the SF history described by the timescale τ (where the SF rate is $SFR \propto \exp^{-t/\tau}$), the age t , the extinction A_V described here by the Calzetti law (Calzetti et al. 2000), and whether or not nebular emission is included. Here we consider three metallicities $Z/Z_\odot = 1, 1/5, 1/20$, a wide range of τ values as well as bursts and $SFR = \text{const.}$, ages up to the Hubble time, and $A_V = 0\text{--}2$ mag. More details on the SED fitting method will be presented in de Barros et al. (2009).

3. Results

3.1. Comparison of SED fits with/without nebular emission

Overall we obtain similar, although not identical, results to E07, when using the same assumptions. In other words, adopting solar metallicity and neglecting nebular emission we find that a significant fraction of the objects (at least 5/10) are best fit by fairly old ages of the order of $t_* \gtrsim 500$ Myr and generally very low extinction. The quality of our fits (expressed in reduced χ^2) is comparable to E07, and similar values are also found for the

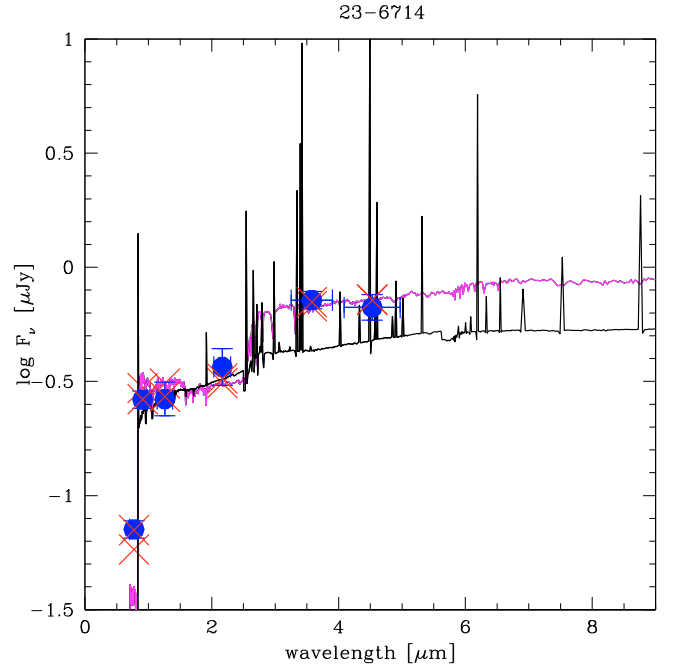


Fig. 1. Observed (blue points) and best-fit SEDs (solid lines) of the $z = 5.83$ galaxy 23_6714 from E07. The errorbars of the observed wavelength indicate the surface of the normalised filter transmission curve. Upper limits in flux indicate 1σ limits. Red crosses show the synthesised flux in the filters. The two SED fits shown are based on a standard Bruzual & Charlot solar metallicity model (magenta), and the same modelling including also nebular emission (black). While the age of the former (with $\chi^2 = 1.61$) is $\gtrsim 700$ Myr, the latter gives $t_* \sim 20$ Myr ($\chi^2 = 0.14$).

stellar masses and current SFR. For example, the mean age, stellar mass, and extinction of the 10 objects we obtain with these assumptions are $\overline{t_*} \approx 500$ Myr, $\overline{M_*} = 1.2 \times 10^{10} M_\odot$, and $\overline{A_V} = 0.11$ (i.e. $\overline{E_{B-V}} \sim 0.05$).

However, including nebular emission changes these results quite drastically. In this case only 1 of 10 objects has a best-fit age $t_* \gtrsim 500$ Myr, and the average age of the sample is lowered by a factor ~ 4 to $\overline{t_*} \approx 120$ Myr. A slightly lower mean stellar mass $\overline{M_*} = 7.8 \times 10^9 M_\odot$ and a higher extinction $\overline{A_V} = 0.34$ ($\overline{E_{B-V}} \sim 0.08$) are also obtained. Compared to the above set of models the χ^2 values is found to be lower for half of the objects. A more rigorous comparison, including also a careful discussion of the uncertainties, is deferred to a later paper.

Examples of SED fits for two objects with known Ly α emission and known spectroscopic redshift are shown in Figs. 1 to 3. Figure 1 shows the best-fit solution using pure stellar SEDs at solar metallicity compared to the best fit including nebular emission (found to be for $Z = 1/5 Z_\odot$). While the age of the latter is $t_* \approx 20$ Myr, the former has an age close to the maximum allowed for the redshift of this object ($z = 5.8$). With nebular emission the apparent Balmer break is mimicked by the presence of strong restframe optical emission lines boosting the flux both in the 3.6 and the 4.5 μm filters³. For this object (23-6714) a non-zero extinction, of $A_V \sim 0.2\text{--}0.8$ depending on metallicity, is required.

¹ See Kotulla et al. (2009) for a comparison of the resulting emission line spectrum with nearby galaxies.

² The emissivities of these lines are known to depend little on n_e and T .

³ The strongest lines in the 3.6 μm filter are [O III] $\lambda\lambda 4959, 5007$ and H β , the strongest at $\sim 4.5 \mu\text{m}$ are H α , [NII] $\lambda\lambda 6548, 6584$, and [S III] $\lambda\lambda 9069, 9532$.

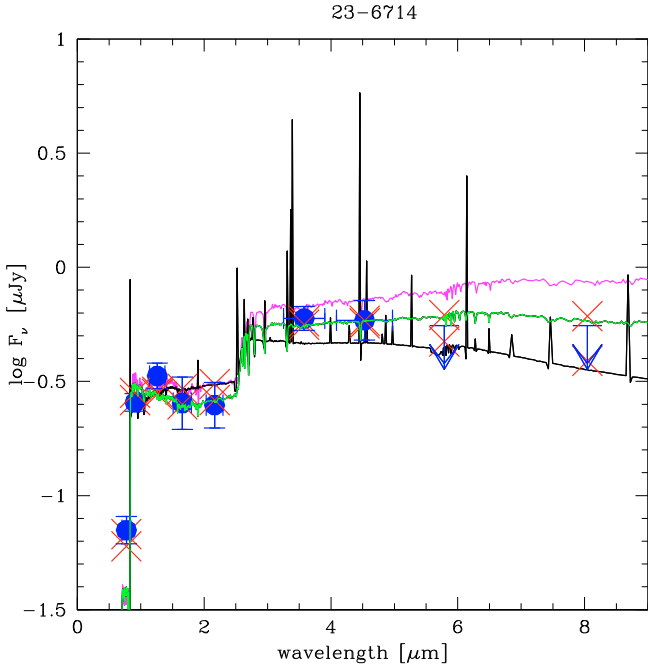


Fig. 2. Same as Fig. 1 for 23_6714, but including IRAC 5.8 and 8.0 μm data (1σ limits), and using the GOODS-MUSIC photometry. The magenta line shows the solar metallicity “standard” SED fit with an old age ($t_\star \gtrsim 700$ Myr) and no extinction obtained in Fig. 1. The black line shows our best-fit including nebular emission with a very young age ($t_\star \sim 6$ Myr) and $A_V \sim 0.7$, the green line the $\gtrsim 700$ Myr best-fit with standard (purely stellar) templates.

Since nebular lines at this redshift are expected to affect the photometry at longer wavelengths ($\gtrsim 5 \mu\text{m}$) less, it is interesting to examine SED fits including the available 5.8 and 8.0 μm data (see Fig. 2). For consistency we therefore use the GOODS-MUSIC photometry in all bands. A good agreement with the observations is found, and again significantly lower ages are obtained with nebular emission. For 23-6714 we find the best fit with $Z = 1/5 Z_\odot$, a very young age of $t_\star \sim 6$ Myr and $A_V \sim 0.7$, compared to ages of $\gtrsim 700$ Myr with standard (purely stellar) templates.

Figure 3 shows an object (31-2185 from E07) with an apparent Balmer break of similar strength. An old age $t_\star \sim 700$ Myr is again obtained here for standard stellar SED fits, whereas the inclusion of nebular emission lowers the age to 90–180 Myr, depending on whether we include or not the photometry in Channels 3 and 4. For this object and for the GOODS-MUSIC photometry, it turns out that nebular emission is not crucial, since relatively short star-formation timescales, hence solutions with few ionising stars, are preferred.

The above results clearly illustrate that it is important to include the effects of nebular emission (lines, in particular) to determine the properties of these high- z galaxies, most importantly their stellar ages.

3.1.1. Comparison with earlier work

Why does this conclusion disagree with E07, who have also examined the possibility of “line contamination” in the IRAC filters, which are crucial to measure the Balmer break or its absence? There are three main reasons. First, E07 compute the contribution of $H\alpha$ to the 4.5 μm filter from an estimate of the unobscured SFR(UV), which assumes a long ($\gtrsim 100$ Myr)

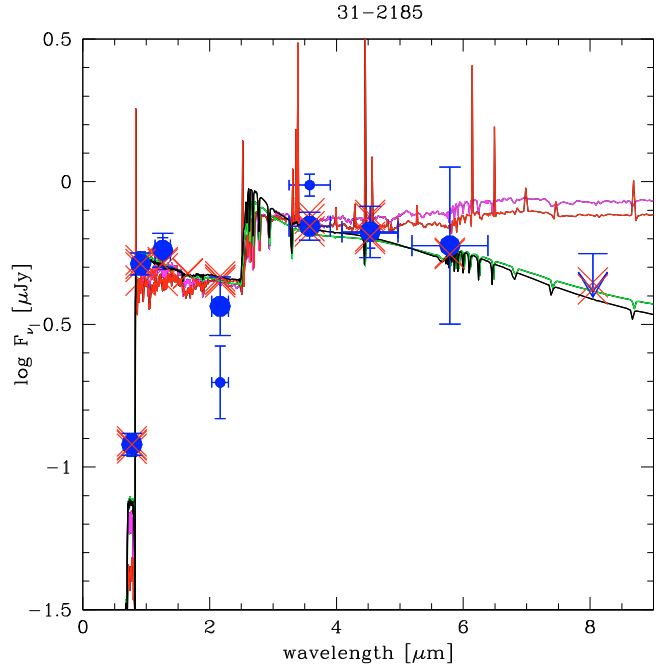


Fig. 3. Same as Fig. 1 for object 31_2185. The two small blue circles illustrate the difference in the photometry of E07 compared to that of the GOODS-MUSIC catalogue shown with large symbols. The red (magenta) line shows the best fit to the photometry of E07 assuming solar metallicity models with (without) nebular emission. The black (green) lines show best fits to the GOODS-MUSIC photometry with (without) nebular emission. For both datasets, the age obtained with nebular emission is $t_\star \sim 90$ –180 Myr, compared to ~ 130 –700 Myr with standard templates.

SF timescale. However, for shorter timescales, the $H\alpha$ luminosity can be higher by up to a factor ~ 4 , as illustrated e.g. by Verhamme et al. (2008, see their Fig. 15). Second, as noted by E07 the contribution of $H\alpha$ is further enhanced when extinction is taken into account. Finally, $[\text{O III}] \lambda\lambda 4959, 5007$ plus $H\beta$ have strong enough intrinsic intensities (typically 1.8–2.2 times $H\alpha$) to also boost the flux in the 3.6 μm filter, thereby mimicking a “Balmer break” between IRAC Channels 1-2 and shorter wavelength filters. When the effects of nebular emission lines are taken into account in a consistent manner with the ionising flux predicted by the SF history, and when extinction is allowed for, we find that – at $z \sim 6$ as considered here – their contribution to IRAC channels 1 and 2 can be significant⁴. This largely explains our lower age estimates than in the earlier work of E07.

3.1.2. How to distinguish “old” and young populations?

Can the two types of SED fits, which explain the Balmer break with “old” stars or by the presence of emission lines, be distinguished observationally? For the SED fit of 23-6714 shown in Fig. 1 for example, the current $SFR \sim 800 M_\odot \text{ yr}^{-1}$. From this the expected $H\alpha$ flux is of the order $3. \times 10^{-16} \text{ erg s}^{-1} \text{ cm}^{-2}$, clearly beyond the reach of current spectroscopic facilities at $\sim 4.5 \mu\text{m}$. Because this object is the brightest of the sample, it appears that direct detections of the restframe optical emission lines need to await future facilities, such as the JWST.

In principle deep photometry at longer wavelengths, where the expected strength of emission lines decreases, could help

⁴ See also the predictions of Zackrisson et al. (2008) who also find significant line contamination even for constant SF over 50 Myr.

disentangle the two solutions. However, the current 5.8 and 8.0 μm data from Spitzer is not deep enough to rule out the “old” SEDs, as shown for the two brightest objects 23-6714 and 31-2185. Although the spectrum of the ~ 700 Myr old population displays an excess with respect to the 5.8 and/or 8.0 μm fluxes, its significance is $\lesssim 2\sigma$ at best. Future, deeper observations should be able to set firmer limits on this issue.

In any case we note that neglecting nebular emission for high- z galaxies with ongoing massive star formation – as testified e.g. by their Ly α emission often used to confirm their redshift spectroscopically – is physically inconsistent, so its effect on the determination of their physical parameters should be taken into account.

3.2. Implications

As shown above, including of nebular emission (lines and continuum) can alter the physical properties of galaxies determined from their SED. For example, by considering just the average properties of our best-fit solutions for the 10 objects fitted here, we obtain $\bar{t}_* \approx 400$ Myr, $\bar{M}_* = 1.1 \times 10^{10} M_\odot$ and $\bar{A}_V = 0.16$ for standard Bruzual & Charlot spectral templates when metallicity is also varied. Including nebular emission we obtain $\bar{t}_* \approx 120$ Myr, $\bar{M}_* = 7.9 \times 10^9 M_\odot$, and a higher extinction $\bar{A}_V = 0.34$. Although this is indicative of the trend obtained with nebular emission, the reader should be aware that large deviations are obtained and uncertainties should be treated properly (cf. Sect. 4).

Clearly the most striking result is that the average age of the $z \approx 6$ galaxies may be decreased typically by a factor ~ 3 compared to earlier studies (cf. Yan et al. 2006; Eyles et al. 2007). Translated to the average redshift of formation z_{form} , this would imply a shift from $z_{\text{form}} \sim 9$. to 6.6, assuming $\bar{z} = 5.873$ for the average redshift of our sample (cf. E07). For only one out of 10 objects do we find best-fit ages of >200 Myr, i.e. a formation redshift beyond 7. If true, this means in particular that the contribution of the galaxies currently observed at $z \sim 6$ to cosmic reionisation must have been negligible at $z \gtrsim 7$, in contrast to the finding of E07.

The average extinction of $A_V \sim 0.34$ mag ($E_{B-V} \sim 0.08$) we find, corresponding to a UV attenuation by a factor ~ 2.2 is also worth noticing. With standard spectral templates, neglecting nebular emission, the average is $A_V = 0.16$. This result indicates that dust attenuation may be stronger than previously thought for Lyman Break galaxies at this redshift. For comparison, Bouwens et al. (2008) assume a UV attenuation factor of ~ 1.5 at $z \sim 6$. If true and representative of the population of $z \sim 6$ galaxies, it may imply an upward revision of the SFR density by $\sim 50\%$. Finally stellar masses, and hence the estimated stellar mass density of i-drop galaxies may also be slightly affected. Also already mentioned, the average stellar mass of our sample \bar{M}_* is $\sim 30\%$ lower when we include nebular emission in the SED fits and leave the other assumptions unchanged.

4. Discussion and conclusions

The main objective of this work has been to examine the effect of nebular emission (lines and continua) on the derivation of physical parameters of $z \sim 6$ galaxies through broad band SED fits. Although our work clearly indicates that this effect can significantly alter derived properties, such as galaxy ages and extinction, we do not (yet) aim at determining absolute values.

Indeed both uncertainties/difficulties in the photometry as well as uncertainties and degeneracies in the models, remain and their effect needs to be quantified properly. For example, the differences obtained using photometry from two sources (revisions) has been illustrated above. Stellar ages and other quantities may also vary if different, more complex SF histories, different extinction laws (possibly also extinction differences between stars and the gas), and different IMFs are allowed in the models.

Last but not least, ours and others SED fitting tools are also limited by their dependence on stellar tracks, which are e.g. sensitive to input physics, such as the treatment of rotation (Vázquez et al. 2007), to the treatment of advanced phases such as TP-AGB stars (cf. Maraston et al. 2006) and others. Once the input physics of the SED fitting code and the photometric data is fixed, errors and degeneracies in the fit parameters need to be quantified in detail and for each individual object. Finally, appropriate quantitative methods should be used to determine the average properties and their uncertainties for samples of galaxies. Such detailed analysis, clearly beyond the scope of this article, will be presented in a forthcoming publication (de Barros et al. 2009).

Independent of these remaining uncertainties, our work shows clearly that the presence of strong Balmer/4000 Å breaks in $z \approx 6$ galaxies is not necessarily caused by stars, but can also be mimicked by restframe optical nebular emission lines, whose contribution to broad band filters increases with $(1+z)$. Apparently “old” ages and high formation redshifts of galaxies with strong ongoing star formation may need to be revised significantly downward. Finally, the impact of nebular emission on the SED analysis of other galaxies, also at lower redshift, also needs to be examined systematically.

Acknowledgements. We would like to thank Matthew Hayes for interesting discussions, Ana Lalovic for the exploration of other SED fits, Roser Pelló for regular discussions and support with *Hyperz*, and David Elbaz for help with GOODS data. This work was supported by the Swiss National Science Foundation.

References

- Anders, P., & Fritze-v. Alvensleben, U. 2003, *A&A*, 401, 1063
 Bolzonella, M., Miralles, J.-M., & Pelló, R. 2000, *A&A*, 363, 476
 Bouwens, R. J., Illingworth, G. D., Franx, M., & Ford, H. 2008, *ApJ*, 686, 230
 Bruzual, G. 2007, in *From Stars to Galaxies: Building the Pieces to Build Up the Universe*, ed. A. Vallenari, R. Tantalo, L. Portinari, & A. Moretti, *ASP Conf. Ser.*, 374, 303
 Bruzual, G., & Charlot, S. 2003, *MNRAS*, 344, 1000
 Calzetti, D., Armus, L., Bohlin, R. C., et al. 2000, *ApJ*, 533, 682
 de Barros, S., Schaerer, D., et al. 2009, in preparation
 Egami, E., Kneib, J.-P., Rieke, G. H., et al. 2005, *ApJ*, 618, L5
 Elsner, F., Feulner, G., & Hopp, U. 2008, *A&A*, 477, 503
 Eyles, L. P., Bunker, A. J., Stanway, E. R., et al. 2005, *MNRAS*, 364, 443
 Eyles, L. P., Bunker, A. J., Ellis, R. S., et al. 2007, *MNRAS*, 374, 910
 Grazian, A., Fontana, A., de Santis, C., et al. 2006, *A&A*, 449, 951
 Ilbert, O., Capak, P., Jalvato, M., et al. 2009, *ApJ*, 690, 1236
 Kotulla, R., & Fritze, U. 2009, *MNRAS*, 393, L55
 Kotulla, R., Fritze, U., Weilbacher, P., & Anders, P. 2009, *ArXiv e-prints*
 Leitherer, C., Schaerer, D., Goldader, J. D., et al. 1999, *ApJS*, 123, 3
 Maraston, C., Daddi, E., Renzini, A., et al. 2006, *ApJ*, 652, 85
 Raiter, A., Fosbury, R., Teimoorinia, H., & Rosati, P. 2009, *A&A*, to be submitted
 Schaerer, D. 2003, *A&A*, 397, 527
 Schaerer, D., & Vacca, W. D. 1998, *ApJ*, 497, 618
 Schaerer, D., & Pelló, R. 2005, *MNRAS*, 362, 1054
 Schaerer, D., Hempel, A., Egami, E., et al. 2007, *A&A*, 476, 97
 Storey, P. J., & Hummer, D. G. 1995, *MNRAS*, 272, 41
 Vázquez, G. A., Leitherer, C., Schaerer, D., Meynet, G., & Maeder, A. 2007, *ApJ*, 663, 995
 Verhamme, A., Schaerer, D., Atek, H., & Tapken, C. 2008, *A&A*, 491, 89
 Yan, H., Dickinson, M., Stern, D., et al. 2005, *ApJ*, 634, 109
 Yan, H., Dickinson, M., Giavalisco, M., et al. 2006, *ApJ*, 651, 24
 Zackrisson, E., Bergvall, N., & Leitert, E. 2008, *ApJ*, 676, L9